ОБЪЕДИНЕННЫЙ
ИНСТИТУТ
ЯДЕРНЫХ
ИССЛЕДОВАНИЙ
ДУБНА

E2-91-562

A.Polanski, A.N.Sosnin, V.D.Toneev

ON ANOMALOUS ^{24}Na PRODUCTION IN HIGH-ENERGY NUCLEAR INTERACTIONS

Submitted to "Атомная энергия"

1991

Introduction

In parallel with a wide investigation of a global mechanism of nucleus-nucleus collisions, allowing one to get some information on a time-space structure of strong interaction processes and properties of nuclear matter far beyond its ground state, the search for phenomena outside the conventional understanding is of unquestionable interest . Over the last years a set of experiments has been carried out by the "calorimetric" technique to investigate the properties of interactions of secondaries produced in relativistic heavy ion collisions (see refs. 1-9 in /1/). The main point in using this method is related to the problem of a possible production of particles with anomalously shortened mean free path in nuclear interactions. Several years ago "the anomalon problem", that is the anomalous fragment production at zero angles, was actively discussed /1/. Some indications of abnormal emission of fragments at relatively large angles have appeared recently. A review of the experimental status of searching for this last effect is given in /2/. In particular, it has been shown that signs of this effect are evident for ^{40}Ar nuclei at energies of about 2 GeV/nucleon but they vanish at energy less than 1 GeV/nucleon. Some difficulties are noted in trying to describe the production of secondary particles and high cross-sections for the large angle ^{24}Na production in terms of conventional theoretical models (see e.g. /3/).

A specific feature of these experiments is the employment of targets and a detector which have a definite thickness and therefore effects of multiple interactions inside the target and the detector are not negligible. In particular, two target-detector configurations are discussed in /2/:

a) Target assembly, consisting of two copper disks 1 cm thick (r=4cm) in "contact" configuration (d=0) and with a gap of 10 cm (fig.1a);

b) Complicated target, consisting of a disk (1cm thick and r=4cm) and a 2π-detector connected to it, which is made of cone rings "cutting out" different angular intervals, and of a second disk placed at a definite distance from the first one (fig.1b).

As was defined in the experiment with two copper disks, the ^{24}Na isotope (half-decay period of about 15 hrs), which possesses a

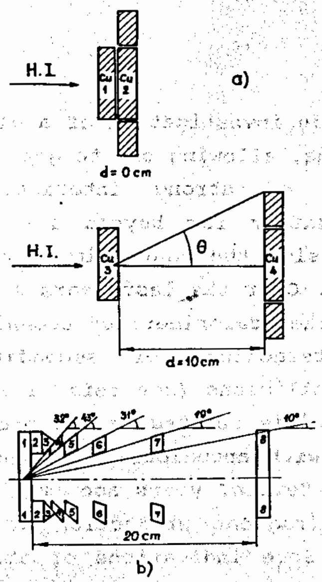

Fig.1 Configurations of the targets discussed in the paper /2/.

stressed γ-line at E_γ=1.3685 MeV is the most convenient for radiochemical experiment. These experiments have shown that the ^{24}Na activity ratio of the first disk to that of the second one depends weakly on the distance between the disks, however, the activity in the second disk goes down when the projectile energy increases (it is seen especially well while comparing experiments at energy 72 GeV of ^{40}Ar ions with experiments at energy 44 GeV of ^{12}C beam). In order to find out the angular dependence of the activity in detail, experiments with a more complicated 2π-detector were carried out.

The relative activity of the 2π-detector elements was compared in /2/ to the results of the Dubna Cascade Model (DCM) calculations of activity induced by fast mesons and nucleons at different angles in interactions of ^{12}C ions (3.65 GeV/nucleon) with copper nuclei. The activity of ^{24}Na fragments in a k-th ring, induced by a particle i at energy E were carried out by using a simple formula, which was referred as a "standard" one in /1/:

$$A_i^k(E) = \sigma_i(E)\ N_i^k(E)\ n_{Cu}, \qquad (1)$$

where $\sigma_i(E)$ - Cu - ^{24}Na cross section of a particle i at energy E; $N_i^k(E)$ - flux of particles i at energy E in an angular interaval corresponding to a k-th ring; n_{Cu} - the number of copper nuclei in 1 cm^3. The values $N_i^k(E)$ are calculated according to the DCM.

A comparison exhibited an essential discrepancy between the experimental and the theoretical activities calculated according to (1), which gave reasons to state that either particles with an abnormally great ability to produce ^{24}Na fragment are available (perhaps, because of abnormally high energy of particles, travelling at large angles), or the DCM predicts too low energy for secondaries at angles greater than 10^o. It should be noted that a direct comparison of the DCM predictions with the results of a "thin target" experiment shows no essential discrepancies in double differential distributions for reactions initiated by ions with mass numbers A $\le$ 40 /4,5/.

If the target extention really influences the spatial, energetic and angular distributions of the particle flux, this influence can be reduced to the following main effects:

particle multiplication in inelastic nuclear interactions in a target and detector causing the deformation of the angular distribution of the particle flux;

ionization losses of primary ^{12}C ions during their transport to the point of their first inelastic interaction;

production of particles with energies exceeding 200 MeV at angles greater than 90^o in the last disk of the detector (so-called albedo effect);

energy losses of particles moving inside the matter block at different angles, which results in a change of the ^{24}Na production cross-section for nuclear interactions of charged particles in the matter (the last effect is really rather small because of the low ionization losses of secondary particles, and it necessarily decreases the resulting activity).

To check the conclusions of /2/ and to discriminate the mentioned media effects, we have carried out calculations of the induced activity by using the "CASCADE" code based on a cascade-evaporation model (CEM) of nucleus-nucleus interactions /4/, supplemented with modules describing the ion and hadron transport in complicated heterogeneous targets and their interactions with the target material /5/.

In short about the model

Over the years of the CEM development quite precise tests of the model accuracy have been carried out for describing the global characteristics of the process of hadron-nucleus and nucleus-nucleus interaction (see refs. /6-7/)*. Let us illustrate the quality of the model description of nucleus-nucleus collisions for the most important characteristics in case of the activation technique under discussion, which are the particle multiplicity and the energy spectra. As an example we consider the data on average energies of the particles (protons and mesons) produced in ^{12}C interactions with the emulsion nuclei /8/, and the emulsion data on charged particle multiplicities in the ^{40}Ar ion reaction /9/. The normalized multiplicity of protons and mesons in the ^{40}Ar + Em

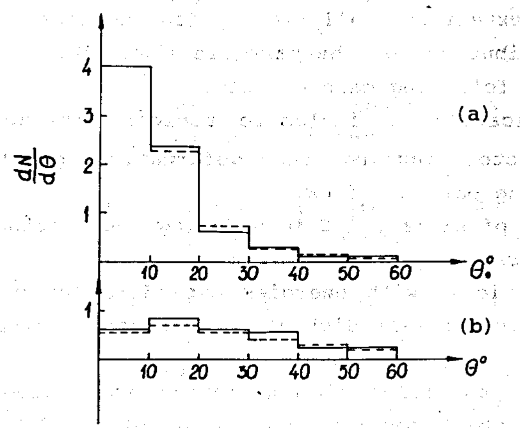

Fig.2 Average multiplicities (relative units) of protons (a) and mesons (b) produced in ^{40}Ar ions interactions with emulsion nuclei (experiment - solid lines) and with ^{64}Cu nuclei (calculation - dashed lines).

interactions (solid line) is compared with the calculated ^{40}Ar + ^{64}Cu results (dashed line) (70 GeV ^{40}Ar ions in both cases) in fig.2. Table 1 shows the data on average proton and meson energy in

---

* The model of nucleus-nucleus interactions used in the present work, is somewhat different from that cited in /3/. For more details see /4-7/.

the ^{12}C + Em (experiment) and ^{12}C + ^{64}Cu (calculation) interactions. It is necessary to stress that in both cases only particles in the velocity region of $\beta > 0.7$ are considered. The cited in Table 1 data, calculated earlier and discussed in /2/, are given for protons and mesons in the energy range from E=50 MeV and higher. It is possible that it is the main cause of the discrepancy noted in /8/ in average proton energies which is just due to experimental acceptance in velocity $\beta > 0.7$ ($\beta = 0.7$ corresponds to a proton energy E=375 MeV). The comparison of the calculated and the experimental data for $\beta > 0.7$ shows good agreement with the exception of the average proton energy in the angle range from θ = 0 to 10^{o}. However it should be remarked that, firstly, it is the incident carbon flux which plays a decisive role in the activity generation in this interval of angles, and, secondly, this discrepancy leads to a decrease of the relative activity of the detector elements. The same agreement is seen for the proton and charged meson multiplicities shown in fig.3. One can see that the model provides quite satisfactory results for the main characteristics of the activation process.

There is a long bibliography list, concerning the CEM (see, e.g., /4-7/ and refs. therein). Therefore, let us discuss in greater detail the simulation technique of the transport and interactions of high energy particles in the target material. To obtain the correct description of the particle transport through the matter, primary attention is centered on the problem of correct description of the competition between two main processes of the interaction of a particle with a matter, i.e. ionization of the material accompanied by consequent losses of particle energy and nuclear interactions resulting in particle multiplication. Transport of a charged particle in the matter leads to a decrease of its interaction energy. The other way round, the rate of inelastic interactions determines the formation of the flux of secondary particles. For particle transport simulation we have chosen the so-called "equalization of particle cross-sections" technique as described in detail in /13/. Inelastic and elastic interaction probabilities are calculated in accordance with the experimental cross-sections. In case of neutral particles the simulation procedure is somewhat easier, because there is no energy dependence on the length of the particle flight in the matter. To describe space configuration of target and detector we use a simplified geometrical module, which differes from those widely used nowadays

Table 1

Average energies of mesons and protons produced with $\beta > 0.7$ at different angles in inelastic interactions of ^{12}C with the emulsion nuclei 3.65 GeV/A.

		$0 - 10^o$	$10 - 20^o$	$20 - 30^o$	$30 - 40^o$
	exper	0.96	0.70	0.60	0.50
π	calc	0.91	0.83	0.56	0.39
	calc /8/*	0.90	0.71	0.50	0.38
	exper	1.8	1.47	1.15	0.9
p	calc	2.9	1.57	0.98	0.82
	calc /8/*	2.4	0.94	0.53	0.74

*Here the data for particles with $T > 50$ MeV corresponding to $\beta > 0.7$ for mesons and $\beta > 0.26$ for protons, are presented.

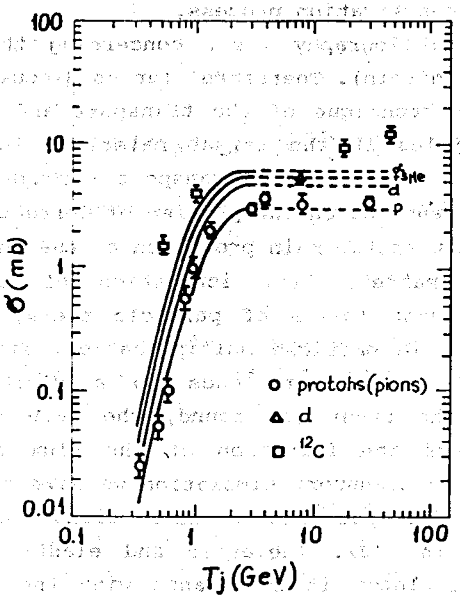

Fig.3 The excitation function for $^{64}Cu(X,Y)^{24}Na$ reaction, according to /2/.

in simulation /14/: a set of geometrical bodies is limited to a cylinder, a cone and a parallelepiped, while the symmetry axes of these bodies must be parallel to the axis in the laboratory system. To describe the geometry of the experiments under discussion this set appears to be suitable.

To test the simulation technique of transport and multiplication of particles in massive targets we carried out calculations /12/, which simulated quite exactly the experimental conditions. In this experiment spectral and angular destributions of neutrons and charged hadrons escaping from the copper cylinder (R=5cm, L=13cm) irradiated by ^{12}C ions with energies 3.65 GeV/nucleon have been measured /10,11/. A good agreement between the calculated and the experimental data for both multiplicity and spectrum distributions of particles confirms the correctness of the developed procedure.

A peculiarity of radioactive nuclei yield calculations is low values for their production cross-sections and the lack of dynamic models, capable of evaluating these cross-sections reliably. That is why the direct simulation method is not effective for evaluation of the relative activity of the detector elements. We used the weight function method when at every inelastic interaction of a particle i with energy E the relative probability of ^{24}Na production in the inelastic interaction is estimated as

$$W_i(E) = \sigma_i^{24Na}(E) / \sigma_i^{in}(E). \quad (2)$$

The available odd data on the cross-sections of ^{24}Na production $\sigma_i^{24Na}(E)$ and their approximations are presented in fig.3 (which is taken from /2/). The cross-sections for π-mesons are assumed to be equal to those for protons $\sigma_\pi^{24Na}(E) = \sigma_i^{24Na}(E)$.

Activity of the k-th ring is then equal to:

$$A_k = \int dE\, W_i(E)\, c_i^k(E), \quad (3)$$

where $c_i^k(E)$ - the collision number of a particle i with energy E in the k-th detector ring, calculated via the MC method.

If the index k=1 corresponds to the angular interval $0 - 10^o$, then the relative activity of any other detector element is equal to

$$R(\theta) = A_k / A_1.$$

These quantities are used in this paper everywhere the calculated relative activity is discussed.

Discussion

The main effects of the matter influence on the particle flux have been noted above. Let us try to estimate how large they are. The calculations show that the ^{12}C ion with energy E=44 GeV passing through 1 cm of copper target loses on the average about several hundreds of MeV until its first inelastic interaction and therefore this energy loss cannot explain the deformation of angular distributions of the secondary particle flux. As to the contribution of particles produced in inelastic ^{12}C + ^{64}Cu collisions and travelling in the backward direction, their multiplicity comes to only 1% of the total particle yield and it is also not a decisive effect.

Tables 2 and 3 show calculation results which not only include the particle production with E > 200 MeV in interactions of

Table 2

Angular dependence of the average hadron multiplicity particles with kinetic energy E > 200 MeV, produced in different stages interaction process.

	Stage	0-10°	10°-20°	20°-30°	30°-40°	40°-50°	50°-60°	ΣN(<60°)
π	I*	197±21	196±14	223±22	164±10	82.5±10	50.6±9	716
π	II	90±14	59±11	77±10	56±7	30±6	26±4	337
π	III	19±4	3±2	5.4±2	3.6±2	1.8±1.7	1.2±0.8	34
(n + p)	I*	967±88	410±23	360±31	226±23	98±12	63±11	2124
(n + p)	II	586±66	205±24	204±14	131±11	67±6	64±11	1257
(n + p)	III	72±9	12±3.5	13±3	7.2±4	2.2±1.2	1.8±1.3	95
n	III	40±9	6.1±2.1	6±2.5	3.8±1.9	1.2±0.9	1.1±0.9	58

* To obtain better statistics the source of secondary particles was summarized over both the front and the end plates of the target. Thus the multiplicity of the secondaries produced in the front plate is roughly one half of that cited in the table.

Table 3

Average energy (GeV) of particles with E > 200 MeV, produced in different stages of interaction process. Statistical uncertainties are shown in brackets.

	Stage	0-10°	10°-20°	20°-30°	30°-40°	40°-50°	50°-60°	<E>,(<60°)
	I	0.94	0.81	0.65	0.49	0.42	0.37	0.68
		(0.06)	(0.05)	(0.03)	(0.02)	(0.02)	(0.02)	
π	II	0.84	0.84	0.66	0.51	0.43	0.36	0.67
		(0.07)	(0.07)	(0.05)	(0.03)	(0.03)	(0.02)	
	III	0.81	0.83	0.62	0.51	0.35	0.37	0.71
		(0.15)	(0.30)	(0.13)	(0.20)	(0.21)	(0.18)	
	I	2.86	1.29	0.80	0.54	0.44	0.40	1.78
		(0.06)	(0.03)	(0.03)	(0.02)	(0.02)	(0.05)	
n + p	II	2.65	1.31	0.84	0.59	0.47	0.40	1.69
		(0.11)	(0.07)	(0.04)	(0.03)	(0.05)	(0.04)	
	III	2.27	1.28	0.95	0.70	0.52	0.43	1.83
		(0.18)	(0.17)	(0.22)	(0.14)	(0.26)	(0.36)	

primaries but also the changes in multiplicity and average energies of produced mesons, nucleons and nuclei, travelling through the target and detector material at different angles. This energy range is of specific interest because it is these particles which make the main contribution to the ^{24}Na fragment production (results of the calculation neglecting inelastic interactions of the first generation particles are given in brackets)*. To elucidate dynamics of the activity formation, we compared the multiplicities and average energy of particles at the following stages of the process:

production of the 1 generation particles due to collisions of incident ^{12}C nuclei (stage I);

characteristics of the particles produced in all subsequent generations crossing the detector ring boundary (stage II);

* Hereafter the incident particles are called particles of zero generation, their "children" belong to the 1 generation, the "children" of the first generation particles - to the second one, etc.

production of the ^{24}Na fragments by these particles in the detector rings (stage III).

First of all let us consider the nucleon channel which is the main source of the detector activity at large angles (see Table 2, stages II and III). It is clearly seen that the multiplicity of the fast particles escaped from the target is higher than that of the first generation particles produced in the target by ^{12}C ions, their angular distributions also differing. Thus, in the first stage the ratio of nucleon multiplicities in angular intervals (10 -20^o) and (20 - 30^o) approaches about 1.15, in the second stage this ratio is equal to 1.0 only (see Table 2). This particle redistribution accompanied by the concerved average kinetic energy defines the activity distribution at different angular intervals (see, stage II for the n + p component in Table 2). It should be pointed out that more than 60 % of activity in nucleonic channel results from neutrons. Evidently, being still in the target volume (i.e. in the first disk) some of the particles of the first generation succeed in interacting to produce particles of the 2 generation. This effect gives on the average about 35% of the multiplicity of the particles, entering the detector at different angles (see Table 2,stages I and II for the n + p component).

We have analysed separately the particle production of different generations. If only primary interactions are considered, the relation of the number of inelastic interactions of the first generation particles to that of zero generation (summated over all angles) attains to about 0.13 (29 and 219 inelastic interactions respectively for the particles of the first and zero generations). Taking into consideration all subsequent generations (summated in both the target and the detector volumes at E > 200 MeV) gives the same ratio 311/117 = 2.65, i.e. about 15 times as high. Recall that in our approach each inelastic interaction contributes to the observed activity. So, it is impossible to speak about an independence of the particle flux and the resulting activity on the spatial size of the target and the detector. Relative angular distributions of particles for primary and secondary inelastic interactions are presented in Table 4. It is seen that the angular distributions of nucleons of the second and subsequent generations are less steep than those of the first generation. This explains at least qualitatively the difference between the activity distributions in the detector rings, estimated by formula (1) when only the first generation particles have been taken into

Table 4

Multiplicity of pions and nucleons of different generations with E > 200 MeV produced in inelastic ^{12}C interactions with ^{64}Cu nuclei (normalised to one inelastic interaction for primary (175) and secondary (256) particles, respectively).

		$0-10^o$	10^o-20^o	20^o-30^o	30^o-40^o	40^o-50^o	50^o-60^o
^{12}C	π	1.0	1.04	0.9	0.83	0.55	0.38
	n + p	4.1	2.2	1.5	1.0	0.59	0.44
Second	π	0.09	0.12	0.16	0.12	0.08	0.06
	n + p	0.5	0.42	0.28	0.21	0.13	0.11

consideration and experimental distribution, which has a specific shoulder in the angular intervals of 10 - 30^o. As for the relative ^{24}Na activity in the 2π-detector elements, our calculation results are presented in Table 5 and in fig.2. One should notice the following purely geometrical peculiarities of the experiment discussed. First of all, the angular intervals "cut out" by the detector rings in the experimental setup, are somewhat different from the theoretically accepted 10^o subdivision. Particularly, in the experiment we have angular intervals from 10 to 19^o, from 19^o to 21^o etc. This difference is the most important for a sharp angular dependence of the particle flux. Moreover, the formula (1) assumes that a particle produced in a definite angular interval should come into an appropriate detector disk. However this is not the case in real geometry of the finite target disk. Depending on an interaction point of a primary particle in the target disk, the displacement along the symmetry axes of the detector for a particle travelling at a definite angle may be as much as 1 cm which does not exclude the possibility of entering the neighbouring rings of the detector. Good agreement in relative activity of the detector rings is seen in fig.4. Comparison between calculated results for the case of particles of the first generation only and the case when all particles in the target and the detector are considered, shows that this difference is not more than 20% and cannot account for the discrepancy between experimental data and calculations

Table 5

Relative activity of the 2π-detector elements bombarded by ^{12}C ions (3.65 GeV/nucleon), %.

	0 – 10°	10 – 19°	19 – 31°	31 – 43°	43 – 52°
exper/1/	100	5.3±0.3	3.6±0.3	0.7±0.3	0.1±0.2
calc	100	4.7±2.7	3.2±2.1	1.0±0.7	0.2±0.15
calc. without younger generations	100	5.7	3.4	1.0	0.2

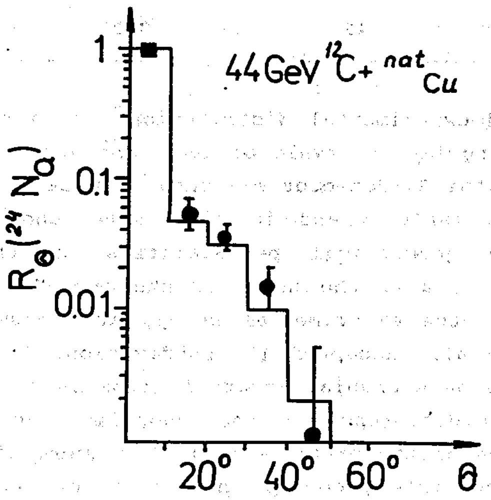

Fig.4 Comparison of calculated and experimental distributions of relative activity: ∘ – experimental data, the histogramm represents the data obtained in our calculations.

according to formula (1). Apparently, the entire set of effects of the charged particle beam interaction with the target and detector material leads to a distortion of angular distributions of the target and detector activity, estimated by the oversimplified formula.

Conclusions

It is shown that the modern understanding of the general mechanism of nucleus-nucleus interactions at energies of several GeV/nucleon allows us to give reliable description of angular and energetic characteristics of the interaction process. Contributions of different generation particles to the formation of the detector activity are determined. A good agreement between calculated and experimental data in relative activity of the detector elements suggests a limited applicability of the standard formula (1) to the conditions of the experiment under discussion. It is quite difficult to indicate a single dominating effect, but as a whole one cannot neglect the influence of finite spatial sizes and geometrical peculiarities of the target and the detector. Therefore, the conclusions of the authors /1/ about the necessity to attract some unusual mechanisms for explaining their experimental results seem to be unconvincing .

We are grateful to Prof. R.Brandt and also to B.A.Kulakov, V.S.Butsev, M.I.Krivopustov G.Haase and m.Heck for fruitful discussions and useful comments.

References

1. R. Brandt et al. JINR Preprint E1-89-803, Dubna, 1989 (revised for submission to Phys. Rev. C, July 1991, private communication).

R. Brandt, V.S.Butsev, H.H.Cui et al. Enhanced Production of ^{24}Na by Wide-Angle Secondaries Produced in the Interaction of Relativistic Carbon Ions With Copper. Proc. X Int. Semin. on High-Energy Physics Problems, 24-29 Sept. 1990, Dubna, p.40.

2. K.Aleklett et al. Phys. Rev. C38,1658,(1988).
3. K.K.Gudima,V.D.Toneev. Jadernaya Fizika, 27,658,(1978).
4. V.D.Toneev et al. Nucl. Phys., A400, 73,(1983).
5. V.S.Barashenkov et al. JINR Preprint P2-83-117, Dubna, 1983.
6. V.S.Barashenkov et al. JINR Preprint P2-85-179,Dubna,1989.
7. V.S.Barashenkov, V.D.Toneev. Interactions of High Energy Particles and Nuclei with Nucleus. Moscow. Atomizdat, 1972, (in Russian).
8. K.D.Tolstov. Z.Physik, A333,(1980),79-82.
9. K.Aleklett et al., Symmetries and Nuclear Structures 13 (1987) Proc. Intern. Sympos. on Symmetries and Nuclear Structures, Dubrovnik, 5. – 14.6.1986, edited by R.A.Meyer and W.Paar, Haarwood Academic Publishers, London, 432, (1987).
10. Bamblevsky V.P. JINR, 16-85-35, Dubna,1985.
11. Alejnikov V.E. et al. JINR Preprint P16-85-97, Dubna,1985.
12. Polanski A.,Sosnin A.N. JINR Preprint P2-87-824,1987.

13. Ermakov S.M., Mikhailov G.A. Statistical Simulation. Moscow. Nauka, 1982.
14. M.B. Emmett et al. GG – the Combinatorial Geometry Module. ORNL-4972, 1975.

Received by Publishing Department
on December 12, 1991.